

# STUDY OF THE PHASE TRANSITION IN $\pi^- C$ INTERACTIONS AT 40 GeV/c

Ts. Baatar<sup>1,3</sup>, B. Batgerel<sup>1</sup>, R. Togoo<sup>1</sup>,  
A.I. Malakhov<sup>2</sup>, B. Otgongerel<sup>1</sup>  
M. Sovd<sup>1</sup>, B. Chadraa<sup>1</sup>, N.G. Fadeev<sup>2</sup>, G. Sharkhuu<sup>1</sup>

- <sup>1</sup> INSTITUTE OF PHYSICS AND TECHNOLOGY, MAS  
<sup>2</sup> JOINT INSTITUTE FOR NUCLEAR RESEARCH, DUBNA  
<sup>3</sup> ULAANBAATAR UNIVERSITY, MSU

Dubna 2012

- 1 PLAN OF THE TALK
  - Introduction
  - Variables used:
  - Experimental method
  - Statistics
- 2  $\pi^- C \rightarrow p + X$  analysis
- 3  $\pi^- C \rightarrow \pi^- + X$  analysis
- 4 DISCUSSION
- 5 CONCLUSION

## Abstract

In this report we are proposed to study the phase transition process to use the new pair for variables  $(T, n_c)$  instead of  $(T, \rho)$  which is mainly used in theoretical calculations and considered the transverse energy spectra of protons and  $\pi^-$ -mesons produced in  $\pi^-C$ -interactions at 40 GeV/c as a function of the cumulative number  $n_c$  (or the four dimensional momentum transfer  $t$ ). Analysis carried out in this paper indicates about the possible appearance of the phase transition of nuclear matter.

# 1. Introduction

The investigation of the multiparticle production process in hadron-nucleus and nucleus-nucleus interactions at high energies and large momentum transfers is very important for understanding the strong interaction mechanism and inner quark-gluon structure of nuclear matter.

During the last years the possibility of the observing of the collective phenomena such as the cumulative particle production [1], the production of nuclear matter with high densities, the phase transition from the hadronic matter to the quark-gluon plasma state is widely discussed in the literature [2-5,11-14].

According to the different ideas and models, if exist these phenomena in the nature, then they will be observed in the hadron-nucleus and nucleus-nucleus interactions at high energies and large momentum transfers and should be influenced to the dynamics of interaction process and would be reflected in the angular and momentum characteristics of the reaction products.

In hadron-nucleus and nucleus-nucleus interactions, in difference from hadron-nucleon interactions, the secondary particles may be produced as a result of multi-nucleon interactions, in other word, the particles are produced in the region kinematically forbidden for hadron-nucleon interactions. This fact is one of the reasons of interest to study the nucleus collision at high energies.

In this paper we are considered the next reactions:



This paper is a continuation of our previous publications [6,7].

## Variables used: 1. Cumulative Number

The cumulative number  $n_c$  in the fixed target experiment is determined by the next formula.

$$n_c = \frac{P_a \cdot P_c}{P_a \cdot P_b} \simeq \frac{E_c - P_{\parallel}^c}{m_p} \quad (3)$$

Here  $P_a$ ,  $P_b$  and  $P_c$  are the four dimensional momentum of the incident particle, target and the considering secondary particles correspondingly.  $E_c$  is the energy and  $P_{\parallel}^c$  is the longitudinal momentum of the considering particle,  $m_p$  is the proton mass. From this formula we see that this variable is a relativistic invariant. This variable ( $n_c$ ) may be interpreted as minimal target mass, which is required for producing of the given secondary particle

because at summarizing by all secondary particles should be obtained the value of the target mass determined on the basis of the energy-momentum conservation law, i.e.

$$M_t \simeq \frac{\sum_{i=1}^n (E - P_{\parallel})_i}{m_p} \quad (4)$$

So,  $n_c$  distribution gives the ordered mass values from the target required for producing of the considering secondary particles. The connection of the variable  $n_c$  and momentum transfer  $t$  is determined by the next formula [7]:

$$t = -Q^2 = (p_a - p_c)^2 = -m_{\pi}^2 - m_c^2 + 2 \cdot E_a \cdot \frac{m_p}{m_p} \cdot (E - p_{\parallel}) \simeq S_{\pi-p} \cdot n_c \quad (5)$$



Where  $S_{\pi-p}$  is the total energy square of  $\pi^-p$  interaction. In this experiment  $S_{\pi-p} \cong 2E_a \cdot m_p \cong 75 \text{ GeV}^2/c^2$  is constant. To study the phase transition of the nuclear matter we must choose the variables corresponding to this physical process. In the theoretical calculations are mainly used the effective temperature  $T$ , the density of nuclear matter  $\rho/\rho_0$  or the chemical potential  $\mu$ . But the variables  $\mu$  and  $\rho$  are not fully determined experimentally. So for studying the phase transition process we must select the other appropriate variable. With this goal let us consider the formula (5) which gives the connection between the variables  $n_c$  and  $t$ . From this formula one can see that with increasing  $t$  the minimal target mass value  $n_c$  which is required from the target for producing of the considering secondary particle increases or vice versa. This means that if any one particle with  $n_c > 1$  (cumulative particle)

is produced in hadron-nucleus interactions at high energies then this particle should be produced at large momentum transfers more than the total energy square of  $\pi^-p$  interaction  $S_{\pi-p}$ , i.e.  $t > S_{\pi-p}$ , for example, if  $n_c = 1.5$  then only for this particle  $t \cong S_{\pi-p} \cdot n_c = 75 \text{GeV}^2/c^2 \cdot 1.5 = 112.5 \text{GeV}^2/c^2$  which is not allowed for  $\pi^-p$  interactions. From the other hand side, if two particles are produced at two different values of  $n_c$  ( $Q_1^2 < Q_2^2$ ), then the size of the particle production region for every particle is different and may be estimated by the formula  $r_1 \sim 1/Q_1$ ,  $r_2 \sim 1/Q_2$  and satisfies the condition  $r_1 > r_2$ , i.e. the size of the particle emission region at high  $Q^2$  is smaller than the case at low  $Q^2$ .

As a result of these two features (increasing of the mass ( $n_c \cdot m_p$ ) and decreasing of the distance  $r$ ) of the variable  $n_c$  (or  $t$ ), the density of the nuclear matter  $\rho$  increases with increasing of  $n_c$ . In this since  $n_c$  (or  $t$ ) is the more appropriate variable to study the phase transition process of nuclear matter. In this case the density of nuclear matter  $\rho$  may be determined by the next formula:

$$\rho = \frac{m}{V} = \frac{n_c \cdot m_p}{V} \quad (6)$$

Where  $V$  is the volume from which the particle is emitted. The volume  $V$  may be estimated as a sphere, i.e.

$$V = \frac{4\pi}{3} r^3 \quad (7)$$

## 2. The effective temperature $T$

The transverse energy spectra of the secondary particles in the different  $n_c$  intervals are approximated by exponential functions of the next form:

$$\frac{1}{2 \cdot E_t} \frac{\Delta N}{\Delta E_t} \sim e^{-b \cdot E_t}, \quad E_t = \sqrt{p_t^2 + m^2} \quad (8)$$

The effective temperature  $T$  is determined as the inverse of the slope parameters  $b$ ,

$$T = \frac{1}{b} \quad (9)$$

## Experimental method

The experimental material was obtained with the help of Dubna 2-meter propane ( $C_3H_8$ ) bubble chamber exposed by  $\pi^-$ -mesons with momentum  $40\text{GeV}/c$  from Serpukhov accelerator. According to the advantage of the bubble chamber experiment, all distributions in this paper are obtained in the condition of  $4\pi$  geometry of secondary particles. The average error of the momentum measurements is  $\sim 12\%$  and the average error of the angular measurements is  $\sim 0.6^\circ$ . All secondary negative particles are taken as  $\pi^-$ -mesons. The average boundary momentum from which  $\pi^-$ -mesons were well identified in the propane bubble chamber is  $\sim 70\text{MeV}/c$ . In connection with the identification problem between energetic protons and  $\pi^+$ -mesons, protons with momentum more than  $\sim 1\text{GeV}/c$  are included to the  $\pi^+$ -mesons. The other experimental details are described in [8,9]

# Statistics

8791  $\pi^-C$  interactions are used in this analysis.

- The total number of protons is 12441.
- The total number of  $\pi^-$ -mesons is 30145.
- $p + C \longrightarrow \pi^- + X$  at  $10\text{GeV}/c$

$$N_{event} = 22510$$

$$N_{\pi^-} = 21470$$

- $p + C \longrightarrow \pi^- + X$  at  $4.2\text{GeV}/c$

$$N_{event} = 8340$$

$$N_{\pi^-} = 3396$$

## 2. $\pi^- C \longrightarrow p + X$

It is interesting to stress that in this experiment the incident particles are  $\pi^-$ -mesons. This means that the secondary protons in  $\pi^- C$  interactions at 40 GeV/c should be produced only in the target fragmentation region, in other words, there is no overlapping from the projectile fragmentation region in the rapidity distribution of protons.

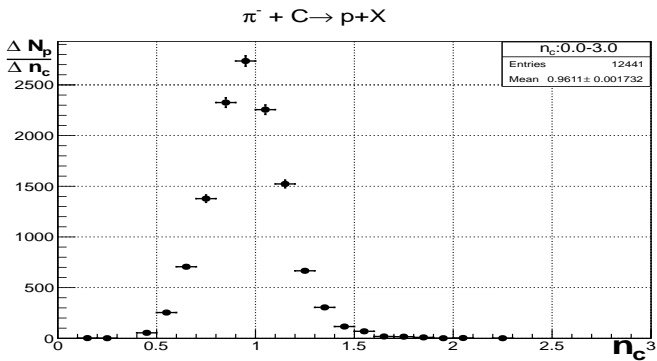


Figure 1: Cumulative number ( $n_c$ ) distribution of protons.

Fig.1 shows the  $n_c$  distribution of the secondary protons produced in  $\pi^- C$ -interactions at  $40\text{GeV}/c$ . From this distribution we see that many protons are produced in the region with  $n_c > 1$  (cumulative protons). This distribution continues until  $n_c \approx 2.3$ .



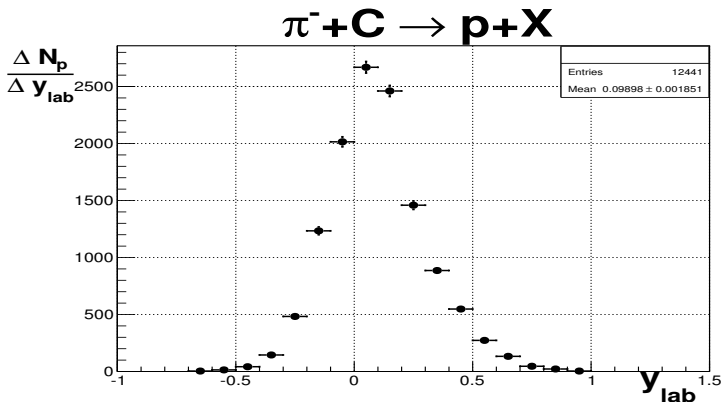


Figure 2: Rapidity distribution of protons.

Fig.2 gives the rapidity ( $y_{lab}$ ) distribution of protons. This distribution shows the protons from  $\pi^- C$ -interactions are produced in the target fragmentation region.

The transverse energy (or transverse momentum) spectrum of the secondary particles produced in hA and AA interactions at high energies may reflect the dynamics of the interaction process more clearly. This is connected with the fact that the transverse effects are mainly generated during the interaction process. In connection with this on Fig. 3(a,b) are shown the transverse energy ( $E_t$ ) spectrum of protons in different  $n_c$ -intervals.

$$\frac{1}{2E_t} \frac{\Delta N}{\Delta E_t} = a \cdot e^{-bE_t}, \quad T = \frac{1}{b}.$$

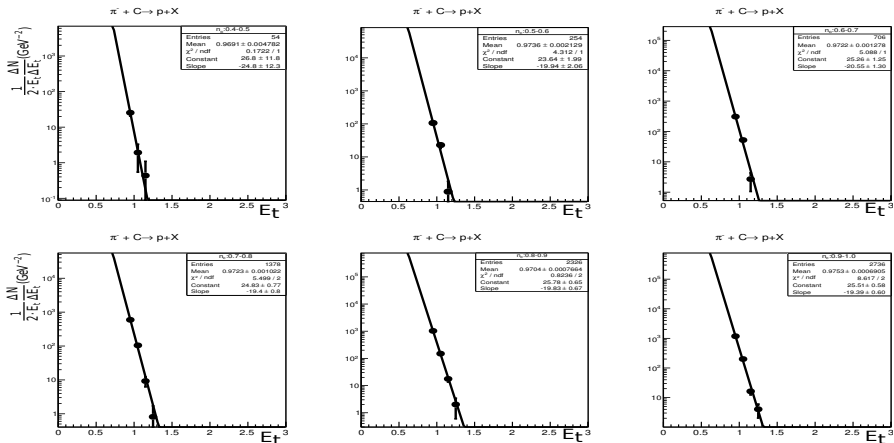


Figure 3.a: Transverse energy  $E_t$  spectrum of protons as a function of different  $n_c$  intervals.

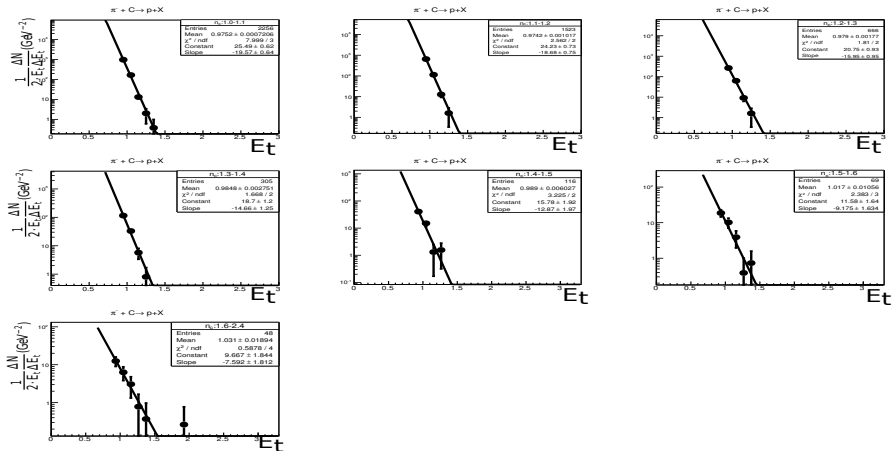


Figure 3.b: Transverse energy  $E_t$  spectrum of protons as a function of different  $n_c$  intervals.

Table 1: The values of the slope parameter  $b$  and the effective temperatures  $T$  on the variable  $n_c$  of protons from  $\pi^- C$  interactions.

$\Delta n_c$	$N$	$b$	$T(\text{GeV})$
0.4 ÷ 0.5	54	$-24.8 \pm 12.3$	$0.040 \pm 0.019$
0.5 ÷ 0.6	254	$-19.94 \pm 2.06$	$0.050 \pm 0.005$
0.6 ÷ 0.7	706	$-20.55 \pm 1.30$	$0.048 \pm 0.003$
0.7 ÷ 0.8	1378	$-19.4 \pm 0.8$	$0.052 \pm 0.002$
0.8 ÷ 0.9	2326	$-19.83 \pm 0.67$	$0.050 \pm 0.001$
0.9 ÷ 1.0	2736	$-19.39 \pm 0.60$	$0.051 \pm 0.001$
1.0 ÷ 1.1	2256	$-19.57 \pm 0.64$	$0.051 \pm 0.001$
1.1 ÷ 1.2	1523	$-18.68 \pm 0.75$	$0.053 \pm 0.002$
1.2 ÷ 1.3	666	$-15.95 \pm 0.95$	$0.062 \pm 0.003$
1.3 ÷ 1.4	305	$-14.66 \pm 1.25$	$0.068 \pm 0.005$
1.4 ÷ 1.5	116	$-12.87 \pm 1.97$	$0.077 \pm 0.011$
1.5 ÷ 1.6	69	$-9.17 \pm 1.16$	$0.108 \pm 0.019$
1.6 ÷ 2.4	48	$-7.59 \pm 1.80$	$0.131 \pm 0.031$

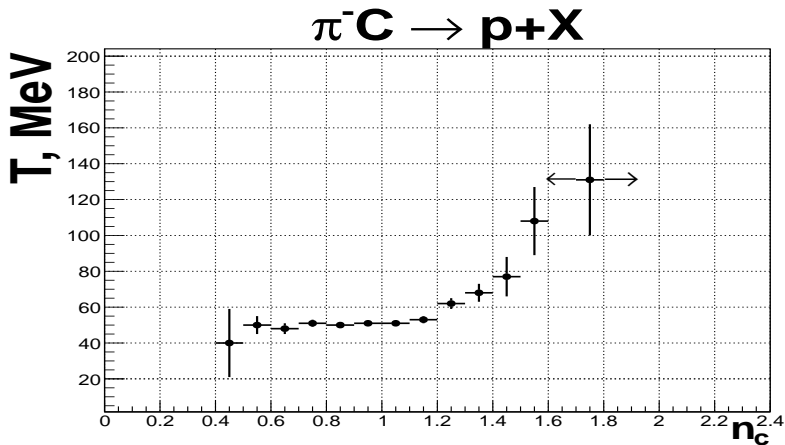


Figure 4: The effective temperature  $T$  of the secondary protons as a function of the variable  $n_c$ .

The experimental spectrum obtained in the every  $n_c$  interval is approximated by the exponential function (8) and the values of the slope parameters  $b$  and the effective temperatures  $T$  on the variable  $n_c$  are shown on Fig.4. Figure 3(a,b), 4 and Table 1 show that the effective temperatures  $T$  are remained practically constant on the level  $T \simeq 50 \text{ MeV}$  until  $n_c \simeq 1.2 \div 1.3$  and then essentially increase.  $T$  may be expressed by Kelvin temperature, then  $T_{\text{plateau}}^p = 50 \text{ MeV} = 0.58 \cdot 10^{12} \text{ K}$ ,  $T_{\text{max}}^p = 131 \text{ MeV} = 1.52 \cdot 10^{12} \text{ K}$  where  $T_{\text{plateau}}^p$  and  $T_{\text{max}}^p$  are the effective temperatures corresponding to region  $n_c^p \leq 1.2$  and  $n_c^p = 1.75 m_p$ . For QGP state QCD predicts  $T \simeq 2 \cdot 10^{12} \text{ K}$ . Now if we suppose the particle is emitted from the spherical volume  $V$  which is determined by the formula (7), then we can give the estimation of the density of the nuclear matter in the  $hA$  interactions at high energies using the formula(6);

$$\rho_{n_c=1.2}^p \rightarrow \frac{1.2 m_p}{V} = \frac{1.2 m_p}{0.082 \text{ fm}^3} = 14.6 m_p / \text{fm}^3,$$

$$\rho_{n_c=1.75}^p \rightarrow \frac{1.75 m_p}{V} = \frac{1.75 m_p}{0.039 \text{ fm}^3} = 44.9 m_p / \text{fm}^3.$$

Where  $\rho_{n_c=1.2}^p$  and  $\rho_{n_c=1.75}^p$  are the estimations of the densities corresponding to the regions  $n_c = 1.2$  and  $n_c = 1.75$

### 3. $\pi^- C \longrightarrow \pi^- + X$

Now we will consider  $\pi^-$ -meson case. Fig.5 presents the cumulative number ( $n_c$ )distribution of  $\pi^-$ -mesons from  $\pi^- C$  interactions at 40GeV/c. This distribution shows  $n_c$  distribution for  $\pi^-$ -mesons continues until  $n_c \simeq 3$ .



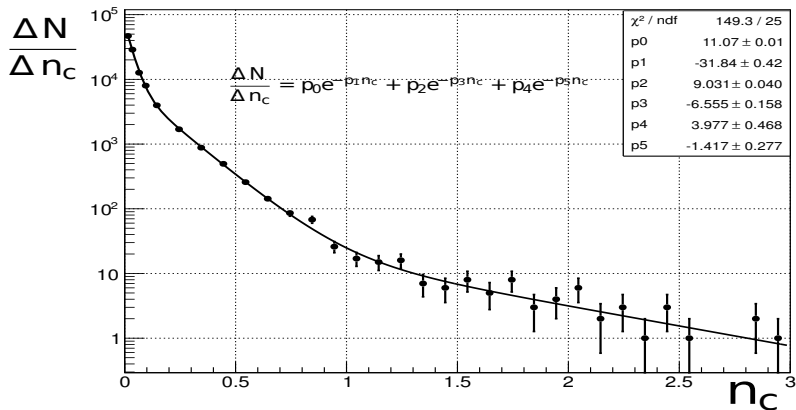


Figure 5: The cumulative number ( $n_c$ ) distribution of  $\pi^-$ -mesons from  $\pi^- C$  interactions. This distribution is well approximated by the sum of three exponential functions with slope parameters  $b_1 = 31.84 \pm 0.42$ ,  $b_2 = 6.555 \pm 0.158$  and  $b_3 = 1.417 \pm 0.277$ .

The rapidity distribution of all  $\pi^-$ -mesons from  $\pi^- C$  interactions is shown in Fig.6. In this experiment the secondary  $\pi^-$ -mesons are produced in the projectile fragmentation, central and target fragmentation regions.

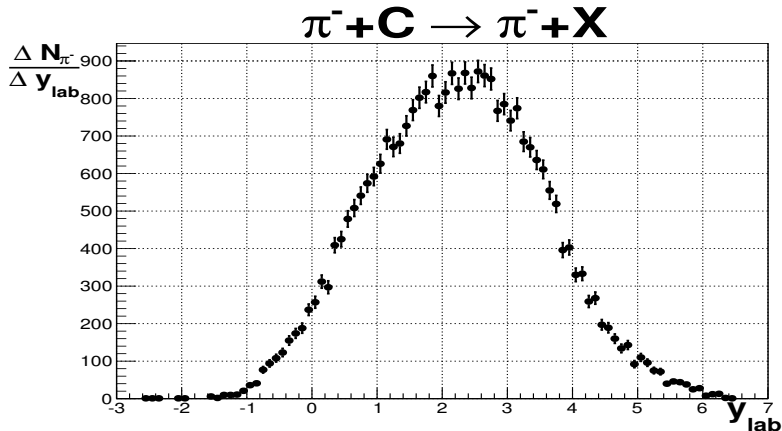


Figure 6: The rapidity distribution of  $\pi^-$ -mesons.

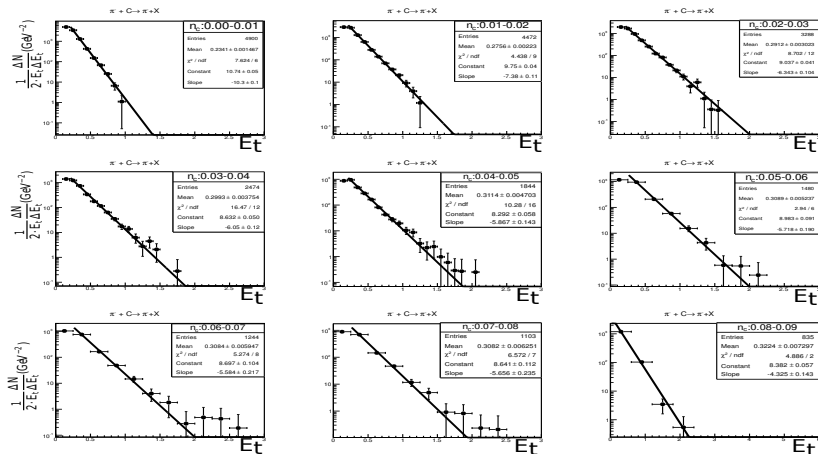


Figure 7(a): Transverse energy  $E_t$  spectrum of  $\pi^-$ -mesons as a function of different  $n_c$  intervals.

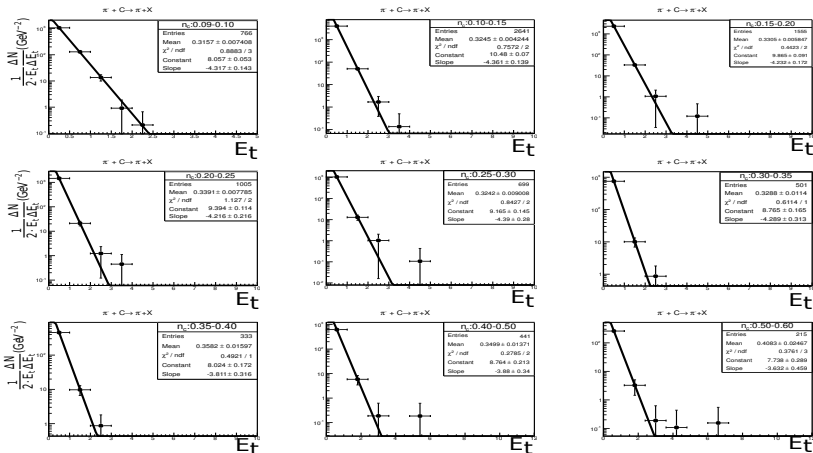


Figure 7(b): Transverse energy  $E_t$  spectrum of  $\pi^-$ -mesons as a function of different  $n_c$  intervals.

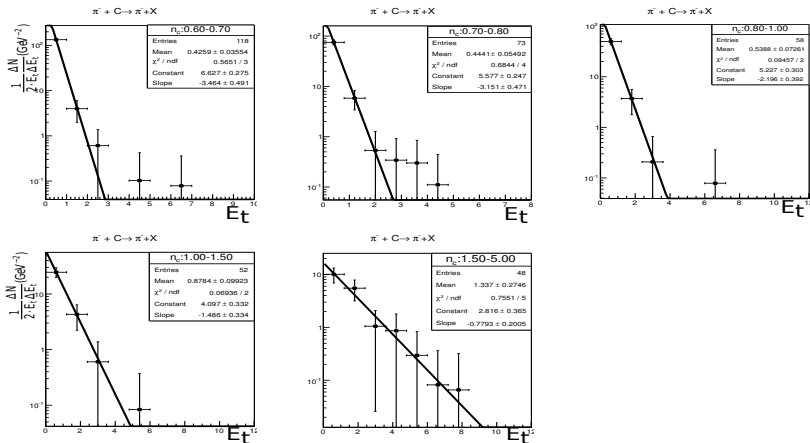


Figure 7(c): Transverse energy  $E_t$  spectrum of  $\pi^-$ -mesons as a function of different  $n_c$  intervals.

Table 2-1: The values of the slope parameter  $b$  and the effective temperatures  $T$  on the variable  $n_c$  of  $\pi^-$ -mesons from  $\pi^- C$  interactions.

$\Delta n_c$	N	$b$	$T, \text{ GeV}$
0.0 $\div$ 0.01	4900	$-10.3 \pm 0.1$	$0.097 \pm 0.008$
0.01 $\div$ 0.02	4472	$-7.38 \pm 0.11$	$0.135 \pm 0.002$
0.02 $\div$ 0.03	3288	$-6.343 \pm 0.104$	$0.157 \pm 0.002$
0.03 $\div$ 0.04	2474	$-6.05 \pm 0.12$	$0.165 \pm 0.003$
0.04 $\div$ 0.05	1844	$-5.867 \pm 0.143$	$0.176 \pm 0.005$
0.05 $\div$ 0.06	1480	$-5.718 \pm 0.190$	$0.181 \pm 0.006$
0.06 $\div$ 0.07	1244	$-5.584 \pm 0.217$	$0.199 \pm 0.012$
0.07 $\div$ 0.08	1103	$-4.656 \pm 0.235$	$0.240 \pm 0.005$
0.08 $\div$ 0.09	835	$-4.325 \pm 0.143$	$0.231 \pm 0.007$
0.09 $\div$ 0.10	766	$-4.317 \pm 0.143$	$0.231 \pm 0.007$
0.1 $\div$ 0.15	2641	$-4.361 \pm 0.139$	$0.229 \pm 0.007$
0.15 $\div$ 0.2	1555	$-4.232 \pm 0.172$	$0.236 \pm 0.009$
0.2 $\div$ 0.25	1005	$-4.216 \pm 0.216$	$0.237 \pm 0.012$

Table 2-2: continued

$\Delta n_c$	N	$b$	$T, \text{ GeV}$
0.25 $\div$ 0.3	691	$-4.39 \pm 0.28$	$0.227 \pm 0.014$
0.3 $\div$ 0.35	501	$-4.289 \pm 0.313$	$0.233 \pm 0.017$
0.35 $\div$ 0.4	333	$-3.811 \pm 0.316$	$0.262 \pm 0.021$
0.4 $\div$ 0.5	441	$-3.88 \pm 0.34$	$0.257 \pm 0.022$
0.5 $\div$ 0.6	215	$-3.632 \pm 0.459$	$0.275 \pm 0.034$
0.6 $\div$ 0.7	118	$-3.464 \pm 0.491$	$0.288 \pm 0.040$
0.7 $\div$ 0.8	73	$-3.151 \pm 0.471$	$0.317 \pm 0.47$
0.8 $\div$ 1.0	58	$-2.196 \pm 0.392$	$0.455 \pm 0.081$
1.0 $\div$ 1.5	52	$-1.486 \pm 0.334$	$0.672 \pm 0.151$
1.5 $\div$ 5.0	48	$-0.7793 \pm 0.2005$	$1.283 \pm 0.330$

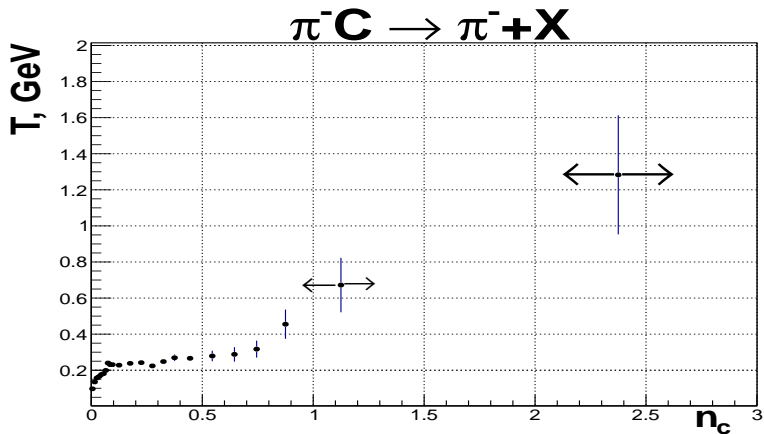


Figure 8: The effective temperature  $T$  of the secondary  $\pi^-$ -mesons as a function of the variable  $n_c$ .



# T, GeV

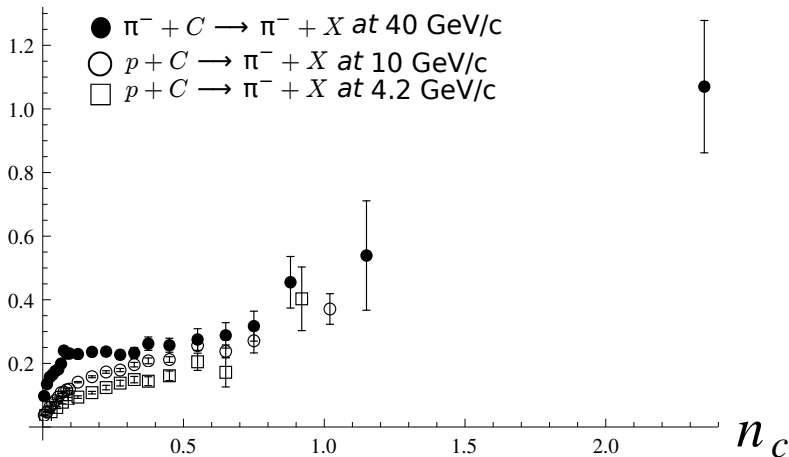


Figure 9: The effective temperature  $T$  of the secondary  $\pi^-$ -mesons as a function of the variable  $n_c$ .

## 4.4. Phase transitions in nuclear physics

203

for  $B^{1/4} = 0.145$  GeV. Note that this value of  $T_c$  is rather low, lower than the transition temperature of 170 MeV obtained by lattice QCD studies. Turning the argument around, for a fixed  $T_c = 170$  MeV, we can obtain the value of  $B^{1/4}$  needed,

$$\begin{aligned} B &= \frac{34\pi^2}{90} T_c^4, \\ B^{1/4} &= 0.236 \text{ GeV}. \end{aligned} \quad (4.222)$$

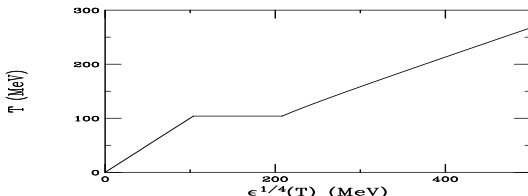


Figure 4.9: The temperature is shown versus energy density in a first-order phase transition with  $T_c = 104$  MeV.

Figure 4.9 shows the one-fourth power of the energy density (x-axis) as a function of temperature (y-axis) for  $T_c = 104$  MeV with  $B^{1/4} = 0.145$  GeV. The transition region is the horizontal line at  $T = T_c$ . The calculation in the hadron phase is shown all the way down to  $T = 0$  although, realistically, for  $T < m_\pi$  the pion mass should be taken into account, as we discuss later. The MeV units on the x-axis are obtained by taking the one-fourth power of the energy density with  $\epsilon$  in units of  $\text{MeV}^4$ . However, the energy density is also often expressed in units

Figure 10: Ultrarelativistic Heavy-Ion collisions.p.203 [14].

## 4. DISCUSSION

Depending on the temperature  $T$  and the variable  $n_c$  (or  $t$ ), the strongly interacting matter may occur in three distinct phases: the hadronic phase, the thermodynamical equilibrium and pure QGP.

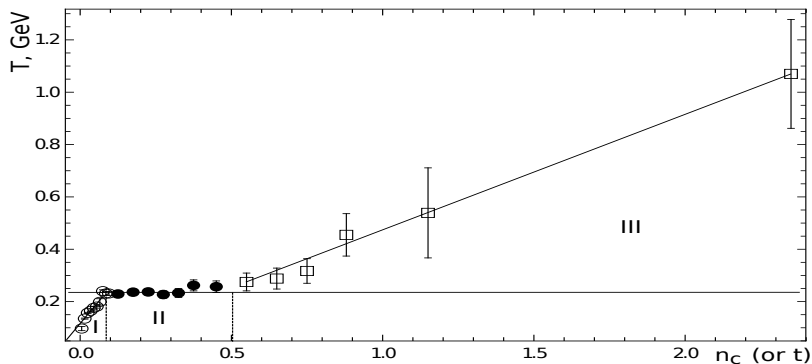


Figure 12: Shows the phase diagram of  $\pi^-$ -mesons produced from  $\pi^-$ -C-interaction at 40GeV/c.

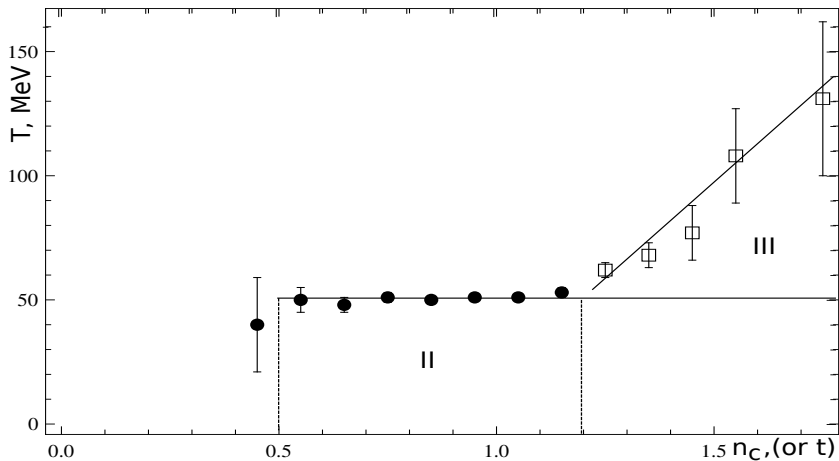


Figure 12: Shows the phase diagram of protons produced from  $\pi^-$ -C-interaction at 40 GeV/c.

Fig.11 and Fig.12 show the phase structure of strongly interacting matter for  $\pi^-$ -mesons and protons produced from  $\pi^-C$ -interaction. So we observe the essential changing of the behaviours of the  $T$ -dependence on the variable  $n_c$  of protons and  $\pi^-$ -mesons from  $\pi^-C$  interactions at  $40\text{GeV}/c$  in two different regions for protons and in three different regions for  $\pi^-$ -mesons. Such behaviours may indicate about the particle production different mechanism in these regions of the variable  $n_c$  (or  $t$ ) and temperature  $T$ . If so, the  $I$  region covered by open circles in which the temperature  $T$  is increased for  $\pi^-$ -mesons (Fig.12) may be connected with the thermalisation of the strongly interacting objects. In this region strongly interacting matter is in the hadronic phase, including highly excited hadrons.

In the // regions covered by black circles (Fig.11 and Fig.12) (nearly quadratic squares) the strongly interacting matter is in the thermodynamical equilibrium phase. In the /// regions covered by open quadratics and with the square of the three angles the strongly interacting matter is in the pure QGP phase.

## 5. CONCLUSION

- The analysis carried out in this paper gives us the possibility to speak about the possible appearance of the phase transition of nuclear matter.
- To study the phase transition processes in  $hA$  and  $AA$  interactions at high energies, the variable  $n_c$  (or  $t$ ) which is used instead of the density of nuclear matter  $\rho$  is a more appropriate variable, in other words, we are proposed to study the phase transition process to use the pair of variables  $(T, n_c)$  instead of  $(T, \rho)$ .
- The strong changing of the characters of the above mentioned dependences may indicate about the particle production different mechanism in these regions. If so, the first region with increasing  $T$  until  $n_c \lesssim 0.1$  may correspond to the thermalisation of the interacting objects (here the strongly interacting matter is in the hadronic phase),

the second region with  $0.1 \lesssim n_c \lesssim 0.5$  for  $\pi^-$ -mesons and with  $0.4 \lesssim n_c \lesssim 1.2$  for protons may indicate about the equilibrium state formation (hadron+QGP state) and the third region with  $n_c \gtrsim 0.5$  for mesons and  $n_c \gtrsim 1.2$  for protons can be connected with the production of pure QGP state.

- Our results show that the numerical characteristics (the temperatures in thermodynamical equilibrium and in the pure QGP state) of phase transition processes for protons and pions are different.
- As a result of the interaction process the strongly interacting matter with different densities is produced and then the secondary particles go out from the nuclear matter with corresponding them density.



## Acknowledgments

First of all we would like to express our thanks to the Dubna two meter propane bubble chamber collaboration members for their excellent experiment and to the Serpukhov accelerator staff for giving  $\pi^-$ -meson beam at 40 GeV/c.

## REFERENCES

- ① Baldin A.M., *Particles and Nuclei.*, 1977, 8, p.429.
- ② J.C. Collins and M.J. Perry., *Phys. ReV. Lett.*, 34(1975), 1353.
- ③ Polyakov A.M., *Phys. Lett. B*59, 1975, 82.
- ④ Polyakov A.M., *Phys. Lett. B*72, 1978, ,477.
- ⑤ Gavani R.V. and Sats H., *Phys. Lett. B*145, 1984, 248.
- ⑥ Baatar Ts.et al., *JINR*, p1-89424, Dubna, 1989.
- ⑦ Baatar Ts.et al., *Journal of Nuclear Physics*, 52, 3(9), 1990.
- ⑧ Balea O. et al., *Phys. Lett. B*39, 571, 1972.
- ⑨ Abdurahmanov A.J. et al., *JINR*, p1-6937, Dubna, 1973.
- ⑩ N. Angelov et al., *JINR* p1-9209, Dubna, 1975.
- ⑪ R.Hagedorn *Nouvo Cim. Suppl.* 3, 147 (1965).
- ⑫ Dirk H. Rischke. *arXiv:nucl-th/0305030v2*.
- ⑬ Baatar.Ts et al., *JINR*, E1-2012-13, Dubna, 2012.
- ⑭ Ramona Vogt, "Ultrarelativistic Heavy-Ion Collisions", Berkeley, CA, USA, 2007.

THANK YOU FOR ATTENTION

# BACK UP

